

## Supplementary Information

# Tuning Copper Sulfide Nanosheets by Cation Exchange Reactions to Realize Two-dimensional CZTS Dielectric Layers

*Ali Hossain Khan,<sup>†</sup> Somnath Pal,<sup>‡</sup> Amit Dalui,<sup>†</sup> Bapi Pradhan,<sup>†</sup> D. D. Sarma,<sup>‡</sup> Somabrata Acharya<sup>\*,†</sup>*

<sup>†</sup>Centre for Advanced Materials, Indian Association for the Cultivation of Science, Jadavpur, Kolkata 700032, India

<sup>‡</sup>Solid State and Structural Chemistry Unit, Indian Institute of Science, Bangalore 560012, India

\*Corresponding author. E-mail: [camsa2@iacs.res.in](mailto:camsa2@iacs.res.in)

### Table of Contents

1. Annealing time variation TEM images of Cu <sub>2</sub> S NSs .....	Fig. S1
2. Ligand controlled TEM images of Cu <sub>2</sub> S NCs .....	Fig. S2
3. Tauc plot of CZTS NSs .....	Fig. S3
4. Moiré interference patterns of CZTS NSs .....	Fig. S4
5. Colloidal solutions of ligand exchange CZTS NSs.....	Fig. S5
6. TEM image of CZTS NSs after ligand exchange .....	Fig. S6
7. HRTEM of the CZTS NSs.....	Fig. S7
8. SAED patterns of the CZTS NSs .....	Fig. S8
9. AFM on the ligand exchanged CZTS NSs .....	Fig. S9

10. XPS survey spectrum of CZTS NSs .....	Fig. S10
11. High resolution XPS spectra of CZTS NSs .....	Fig. S11
12. TEM image & EDS spectrum Tin doped Cu <sub>2</sub> S NSs .....	Fig. S12
13. Precursor tuned EDS compositions.....	Table S1
14. Cation exchange with equal mole of Zn and Sn salts.....	Fig. S13
15. Cation exchange in presence of oleylamine .....	Fig. S14
16. Cross-sectional SEM image of dielectric device.....	Fig. S15
17. Dielectric comparison of CZTS NSs with established dielectric materials.....	Table S2
18. Impedance parameters at different temperatures.....	Table S3
19. AC conductivity vs 1/T plots at different frequencies.....	Fig. S16

### Supplementary Information Figures

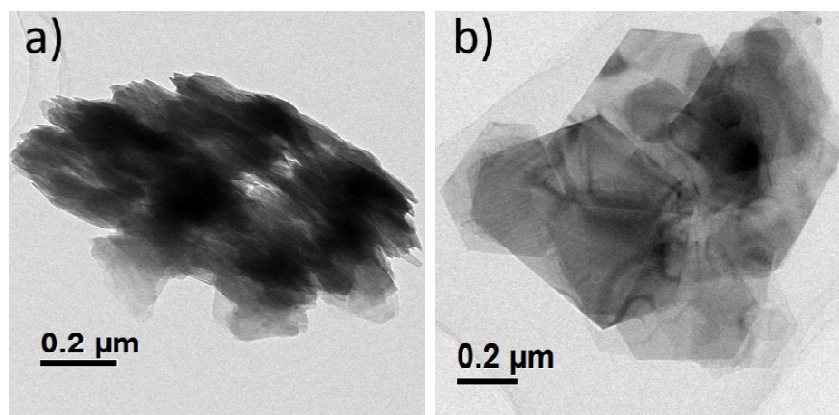


**Fig. S1** TEM images of Cu<sub>2</sub>S NSs synthesized at 240°C with annealing time of (a) 10 mins and (b) 60 mins.

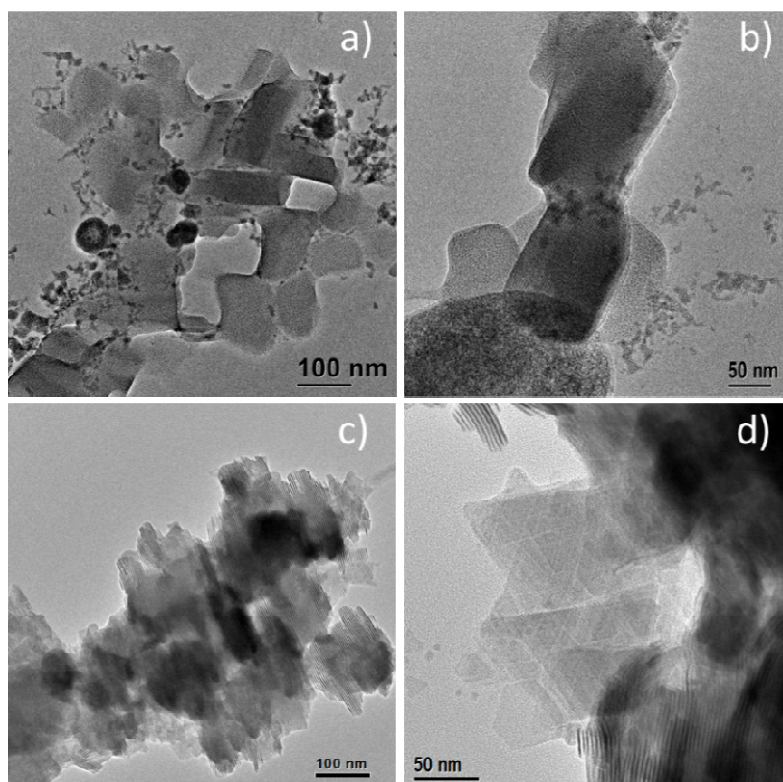


**Fig. S2** TEM images of  $\text{Cu}_2\text{S}$  NCs synthesized at  $240^\circ\text{C}$  (a, b) without TOPO and (c, d) without oleic acid.

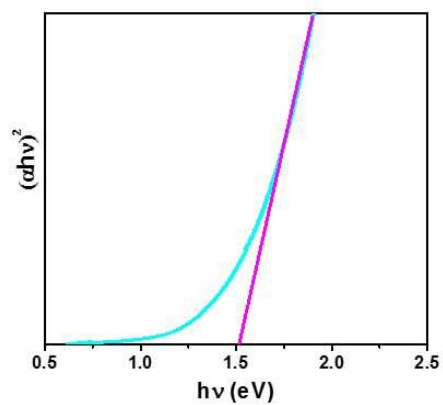


**Fig. S3** Tauc plot of CZTS NSs for the determination of band gap threshold of the synthesized NS. The band gap energy of CZTS NSs has been determined from the UV-vis spectrum to be 1.50 eV by extrapolation of the linear region of a plot of  $(\alpha hv)^2$  versus photon energy ( $h\nu$ ), where  $\alpha$  represents the absorption coefficient.

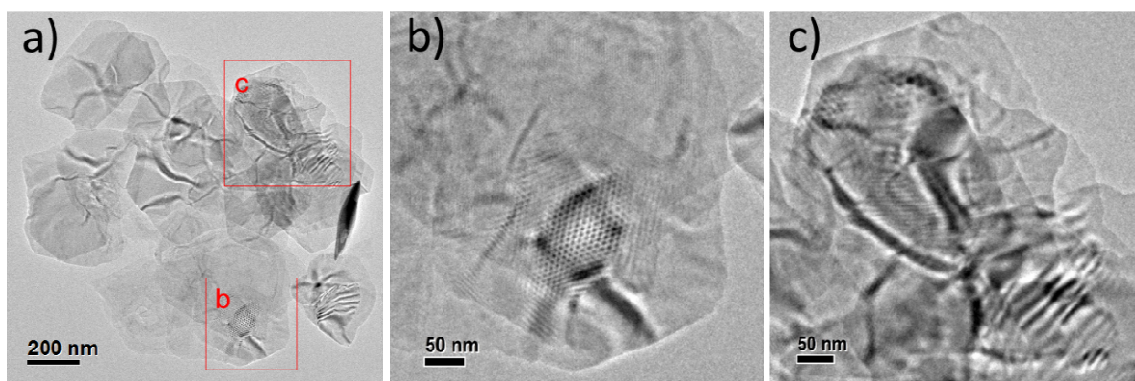


**Fig. S4** (a) TEM image of CZTS NSs. (b, c) Magnified areas of CZTS NSs showing Moiré pattern for the overlapped NSs with rotational offsets of the crystal lattice.

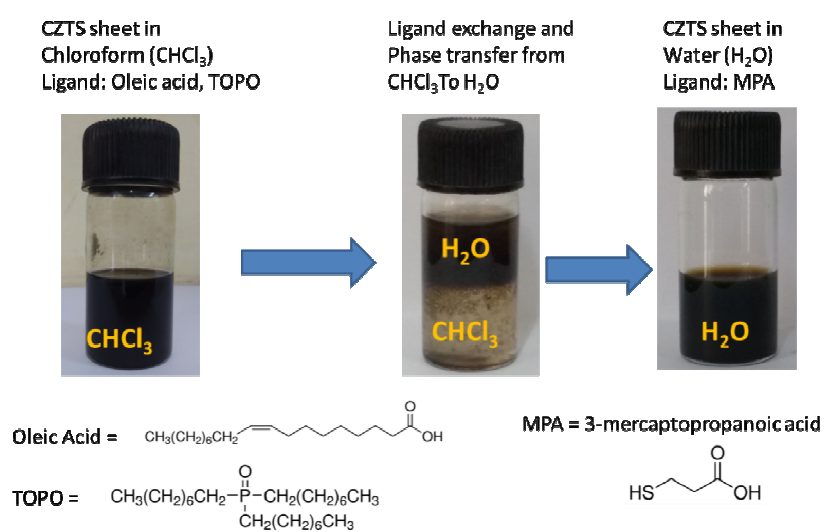


**Fig. S5** Photograph of colloidal solutions showing the ligand exchange and phase transfer process of CZTS NSs from chloroform to water.

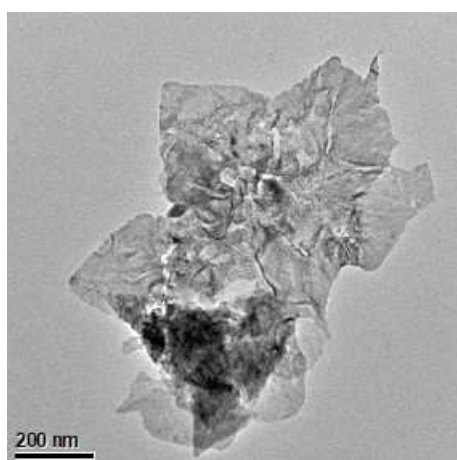


**Fig. S6** TEM image of CZTS NSs after ligand exchange.

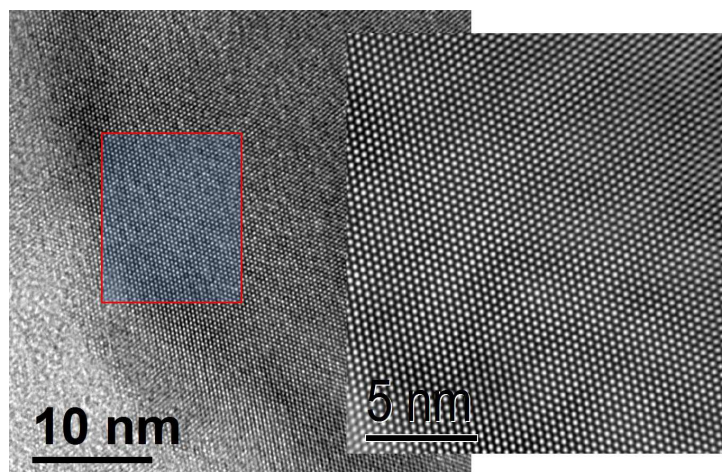


**Fig. S7** HRTEM image of a single CZTS NS showing the well resolved atoms indicating the single crystalline nature of the NS.

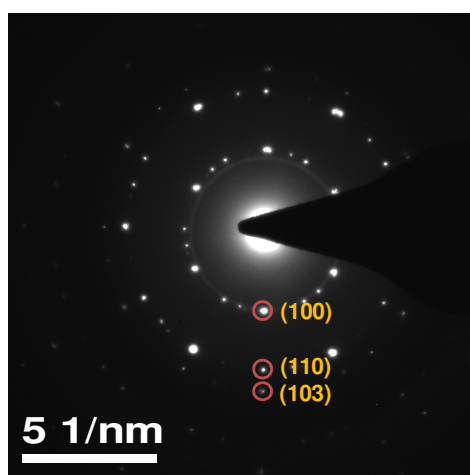


**Fig. S8** SAED pattern of the CZTS NSs, which is showing the diffraction spot corresponding to reflection of different planes of wurtzite crystal structure.

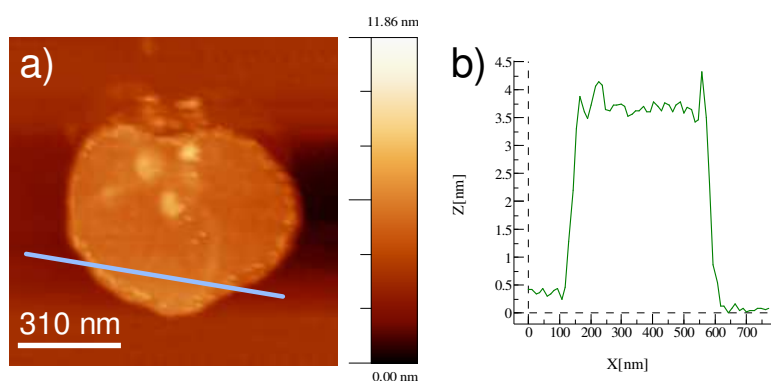


**Fig. S9** (a) Tapping mode AFM image of the ligand exchange CZTS nanosheets. (b) Height profiles obtained from the AFM image along the cyan line.



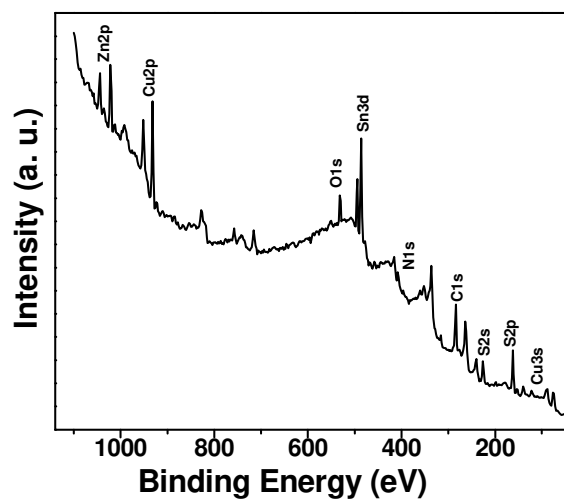


**Fig. S10** X-ray photoelectron survey spectrum of the CZTS NSs showing the different constituent elements present within the NSs.

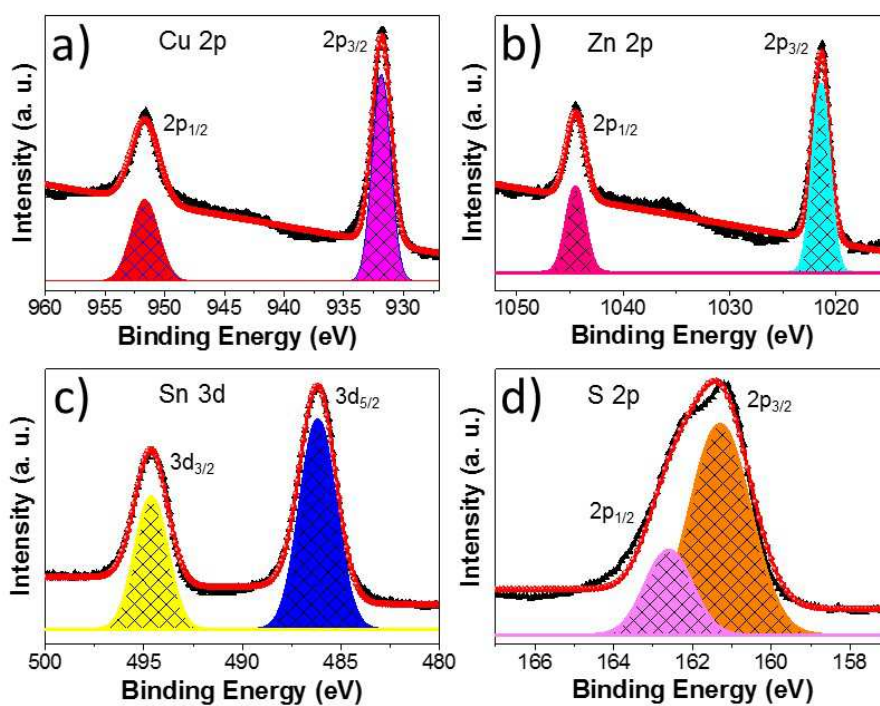


**Fig. S11** High-resolution XPS spectra of (a) Cu, (b) Zn (c) Sn, and (d) S of CZTS NSs.

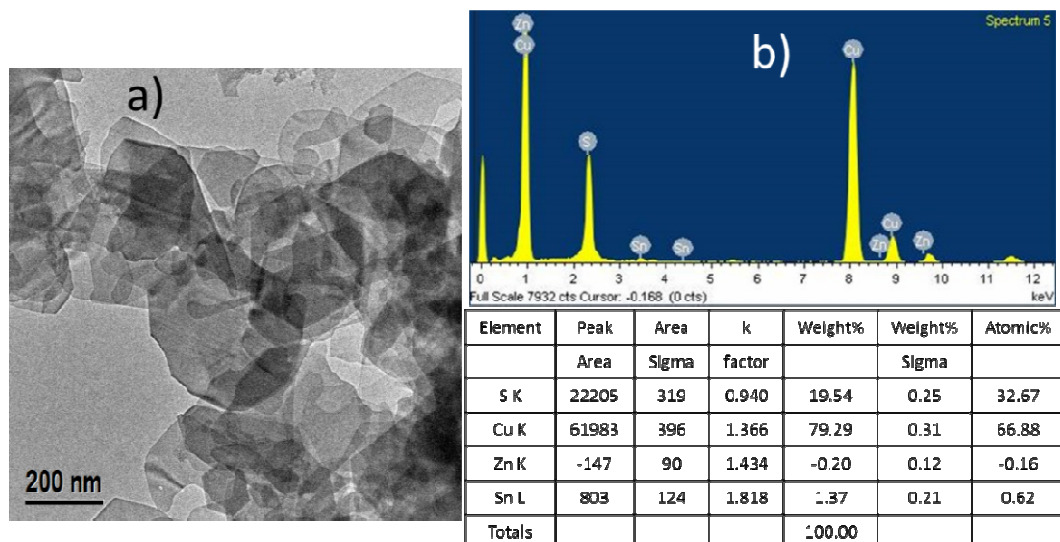


**Fig. S12** (a) The TEM image and (b) EDS spectrum and elemental analysis of Tin doped  $\text{Cu}_2\text{S}$  NSs synthesized via one pot synthesis (following the  $\text{Cu}_2\text{S}$  NSs preparation procedure) using the 2:1:1 mole ratio of Cu(I)/Zn(II)/Sn(IV).

**Table S1** Amount of precursors used for the cation exchange reaction and the final composition of the ions in the NSs.

$\text{Cu}_2\text{S}$ NSs (mmole)	Zn(OAc) (mmole)	ZnCl <sub>2</sub> (mmole)	Zn(acac) <sub>2</sub> (mmole)	SnCl <sub>4</sub> (mmole)	SnCl <sub>2</sub> (acac) <sub>2</sub> (mmole)	Zn:Sn used	Ligands used	TEM grid used	S:Cu:Zn:Sn from TEM-EDS
0.5	0.25	--	--	0.25	--	1:1	0.5mL DDT	Au	44 : 37 : 1 : 18
0.5	--	0.25	--	0.25	--	1:1	0.5mL DDT	Cu	35 : 56 : 0.33 : 8
0.5	--	1.5	--	0.25	--	6:1	1mL DDT	Cu	39 : 42 : 3 : 16
0.5	--	0.0625	--	--	0.25	1:4	0.5mL OLA	Cu	25 : 56 : 18 : 3
0.5	--	0.05	--	--	0.3	1:6	0.5mL OLA	Au	43 : 36 : 15 : 7
0.5	--	--	0.03	--	0.3	1:10	0.5mL OLA	Au	49 : 32 : 10 : 9
0.5	--	--	0.03	--	0.322	1:10.7	0.5mL OLA	Au	49 : 32 : 11 : 9
0.5	--	--	0.04	--	0.4	1:10	0.5mL OLA	Au	49 : 27 : 11 : 12

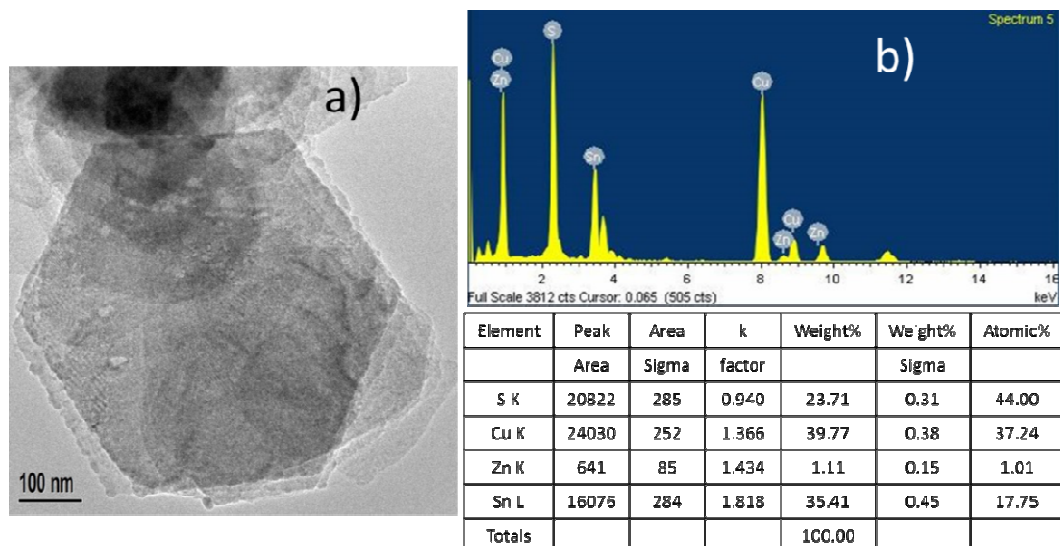


**Fig. S13** (a) The TEM image and (b) EDS spectrum and elemental analysis of CZTS NSs synthesized by cation exchange of  $\text{Cu}_2\text{S}$  NSs with equal amounts (moles) of Zn and Sn in the presence of DDT.

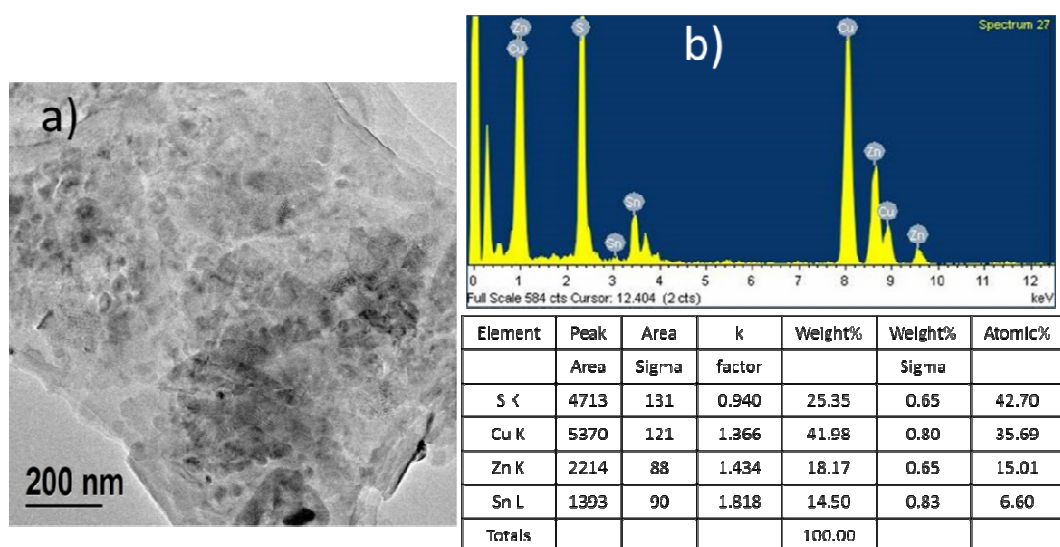


**Fig. S14** (a) The TEM image and (b) EDS spectrum and elemental analysis of CZTS NSs synthesized by cation exchange of  $\text{Cu}_2\text{S}$  NSs in the presence of oleylamine.



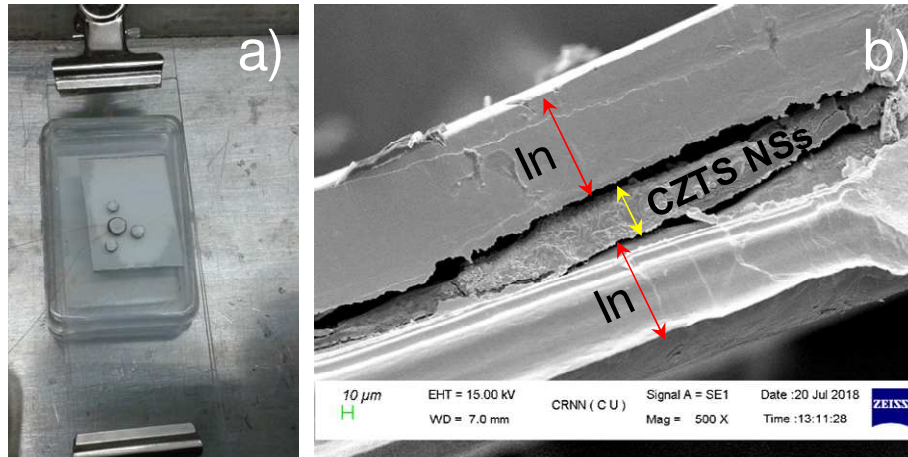


**Fig. S15** (a) Device picture and (b) the cross-sectional SEM image of In-CZTS NSSs-In dielectric device, showing ~50  $\mu\text{m}$  thick CZTS layer between two Indium (In) plate.

**Table S2** A comparison of dielectric properties of established dielectric materials with 2D NCs of CZTS.

Composition	$\epsilon'$	D or $\tan(\delta)$ (100 kHz) at 300 K	$\text{TC}_{\epsilon'}$ ( ppm/K) 100 kHz at 300 K
$\text{TiO}_2$ [S1]	110	0.015	(-)750
$\text{SiO}_2$ [S1]	3.7	0.0015	-
$\text{CaTiO}_3$ [S1]	130	0.11	(-)1600
$\text{SrTiO}_3$ [S1]	285	0.006	(-)2400
$\text{MgO}$ [S1]	10	0.001	(+)190
$\text{MgTiO}_3$ [S1]	16	0.02	(+)100
$\text{Al}_2\text{O}_3$ [S1]	10	0.002	(+)120
$\text{BaTi}_4\text{O}_9$ [S2]	37	0.0015	(-)110
$\text{Ta}_2\text{O}_5$ [S3]	35	0.006	(+)600
$\text{Bi}_2\text{Zn}_{1/3}\text{Nb}_{2/3}\text{O}_7$ [S2][S4]	80	0.001	(+)150
$\text{HfO}_2$ [S5]	26	0.1	(+)300 to (+) 600
$\text{Ho}_2\text{CuTiO}_6$ [S6]	53	0.005	(-)64
$\text{PbS}$ [S7]	13	0.0012	(+) 51
CZTS	6.1	0.03	600

**Table S3** Fitted results of impedance parameters at different temperatures.

Temperature (K)	R <sub>1</sub> (Ohm)	CPE <sub>1</sub> (F)	CPE <sub>1</sub> -( $\alpha$ )	R <sub>2</sub> (+)	CPE <sub>2</sub> (F)	CPE <sub>2</sub> -( $\alpha$ )
280.095	2.289E+09	6.244E-12	1	9.992E+07	1.994E-10	0.87968
290.065	1.469E+09	7.260E-12	1	2.573E+07	5.272E-11	0.93947
300.035	7.794E+08	8.419E-12	0.9886	1.570E+07	3.426E-11	0.97592
310.095	3.942E+08	8.808E-12	1	1.596E+07	2.678E-11	0.96032
320.14	2.304E+08	1.011E-11	0.99739	1.419E+07	2.141E-11	0.96561
330.21	1.476E+08	1.167E-11	0.99307	1.280E+07	1.845E-11	0.96909
340.535	1.012E+08	1.307E-11	0.98571	1.001E+07	1.719E-11	0.97355
350.23	7.449E+07	1.435E-11	0.97947	8.308E+06	1.652E-11	0.9758

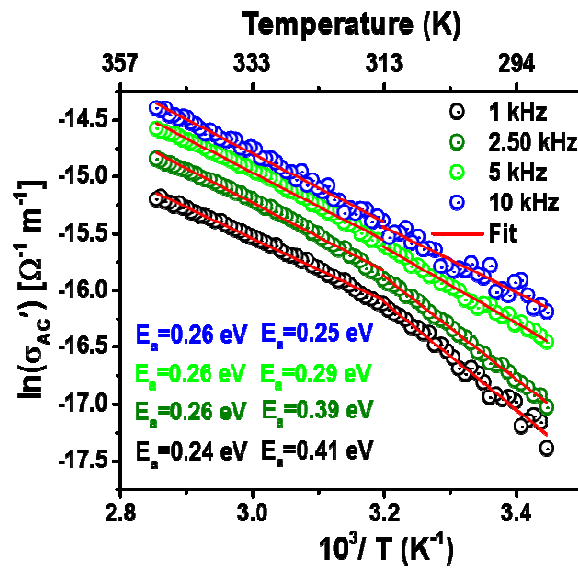


**Fig. S16** AC conductivity ( $\sigma'_{AC}$ ) versus reciprocal of temperature ( $1/T$ ) plots at different frequencies suggests that the activation energy decreases both at lower and higher temperatures with increasing frequencies.

#### References

- S1 G. D. Wilk, R. M. Wallace and J. M. Anthony, *J. Appl. Phys.*, 2001, **89**, 5243-5275.
- S2 M. B. Telli, S. Trolier-McKinstry, D. I. Woodward and I. M. Reaney, *J. Sol-Gel Sci. Technol.*, 2007, **42**, 407-414.
- S3 A. I. Kingon, J. P. Maria and S. K. Streiffer, *Nature*, 2000, **406**, 1032-1038.
- S4 S. Kamba, V. Porokhonsky, A. Pashkin, V. Bovtun, J. Petzelt, J. C. Nino, S. Trolier-McKinstry, M. T. Lanagan and C. A. Randall, *Phys. Rev. B*, 2002, **66**, 054106.
- S5 J. Zhu, Z. G. Liu and Y. R. Li, *J. Phys. D: Appl. Phys.*, 2005, **38**, 446.

- S6 D. Choudhury, A. Venimadhav, C. Kakarla, K. T. Delaney, P. S. Devi, P. Mondal, R. Nirmala, J. Gopalakrishnan, N. A. Spaldin, U. V. Waghmare and D. D. Sarma, *Appl. Phys. Lett.*, 2010, **96**, 162903.
- S7 A. H. Khan, S. Pal, A. Dalui, J. Pradhan, D. D. Sarma and S. Acharya, *Chem. Mater.*, 2017, **29**, 1175-1182.